Proceedings of the Canadian Society for Mechanical Engineering International Congress
32nd Annual Conference of the Computational Fluid Dynamics Society of Canada
Canadian Society of Rheology Symposium
CSME/CFDSC/CSR 2025
May 25–28, 2025, Montréal, Québec, Canada

Representative Driving Cycle Construction Incorporating Road Grade Transitions Using A Markov-chain Method.

Amirreza Yasami[1*], Mohamadali Tofigh[1], Mahdi Shahbakhti[1], Charles Robert Koch[1]

[1]Department Mechanical Engineering, University of Alberta, Edmonton, Canada
[*] ayasami@ualberta.ca

February 12, 2025

***Abstract*—**Driving cycles are needed for vehicle design, fuel economy analysis, and transportation emission estimation. Despite their significant role, conventional driving cycle construction methods often fail to capture the full range of real-world driving dynamics, primarily due to their limited consideration of road grade. In this work, a Markov Chain-Based (MCB) methodology for constructing representative driving cycles is presented, which integrates extensive real-world data, including vehicle speed, acceleration, and road grade. By leveraging a sparse transition matrix, our proposed approach enhances computational efficiency and is scalable to large state spaces. Experimental evaluations demonstrate that incorporating road grade significantly improves driving cycle representativeness, with the mean Vehicle Specific Power (VSP) changing from 1.45 to 1.44 kW/tonne (a 0.69% decrease), variance increasing from 4.29 to 6.15 (a 43.3% increase), and the maximum VSP rising from 7.53 to 11.6 kW/tonne (a 54.2% increase). Quantitative assessments further demonstrate that while average speed and acceleration errors are maintained within 8.31% and 6.03%, respectively, idling time is underestimated by 68.7% compared to the experimental data, which is a potential area for future refinement. Overall, the results underscore that the representative driving cycle incorporating vehicle speed, acceleration, and road grade provides a better foundation for accurate performance evaluations and emissions analyses. Future research will focus on further optimizing computational efficiency and extending the framework to account for additional variables such as weather conditions and cold climate effects, helping to contribute to the advancement of next-generation, eco-friendly transportation systems.

***Keywords-component*—Representative Driving Cycle; Markov-chain; Road Grade; Vehicle Specific Power.**

This work was supported by Energy Management and Sustainable Operations (EMSO) of the University of Alberta and Environment and Climate Change Canada, under the Climate Action and Awareness Fund. (*sponsors)*

I. INTRODUCTION

Climate change remains a significant global challenge, impacting the environment, public health, and economic stability [1]. Fossil fuel consumption, particularly from coal, oil, and gas, accounts for over 75% of global greenhouse gas (GHG) emissions and nearly 90% of carbon dioxide emissions [2]. The transportation sector alone contributed 7943 Mt CO_2 eq in 2022, comprising 20% of global emissions and reflecting a 22% increase since 2005 [3]. In Canada, transportation is the second-largest emitter, responsible for 28% of national GHG emissions, with an observed 3% rise from 2005 to 2022 [4].

Governments worldwide have introduced stringent regulations and emission standards to curb vehicle emissions [5], [6]. These policies have accelerated research on advanced vehicle technologies, emission estimation models, and clean power generation systems [7]. The further development of representative driving cycles is needed to accurately analyze fuel consumption and emissions under real-world conditions [8], [9]. Standardized "type-approval" tests fail to reflect actual driving behaviors, leading to discrepancies between manufacturer-certification results and real-world fuel economy and emissions [10]. Thus, local driving cycles tailored to specific regions are essential to evaluate and improve emission reductions in vehicular systems [11], [12].

Multiple methodologies have been proposed for constructing representative driving cycles, including micro-trip-based (MTB) methods, cluster-based approaches, and Markov-chain-based (MCB) techniques [13]–[15]. However, each method has limitations. MTB methods, which segment driving data into micro-trips and randomly sample them to construct a cycle, are widely used due to their simplicity [16], [17]. However, they

produce discontinuous acceleration and grade profiles [18] and are ineffective in scenarios with minimal stops, such as highway driving [19].

MCB methods, employ a transition probability matrix (TPM) to model the likelihood of transitioning between different driving states [20], [21]. These states, defined by parameters such as speed and acceleration, are derived from real-world driving data and used to generate representative cycles via the Monte Carlo method. MCB techniques preserve the statistical characteristics of real-world driving conditions more effectively than MTB methods but have an extensive state space, making them computationally intensive [19]. Augmenting factors such as road grade, further increases the complexity [22].

Road grade is typically an important factor influencing fuel consumption and emissions in real driving, yet it is often overlooked in representative driving cycle studies [23]. Studies show that road grade contributes between 1% and 9% of fuel consumption for commercial vehicles and up to 40% for specific real-world conditions [24].

A method for constructing multi-dimensional representative driving cycles by incorporating road grade transitions in the experimental data via an improved MCB method is presented. To validate the methodology, an extensive dataset was collected from on-road experiments over 2100 kilometers. The main contributions of this study are:

- An extensive dataset from 105 real-world driving tests conducted with a 2021 Plug-in Hybrid Ford Escape in Edmonton, Alberta, Canada. This dataset provides the foundation for our analysis.
- A Markov-chain-based (MCB) approach is developed that integrates road grade transitions directly from the experimental data, yielding a three-dimensional framework that enhances the accuracy of the driving cycle construction.
- How the inclusion of road grade influences the constructed representative driving cycle by examining the effects on driving cycle fidelity and potential implications on vehicle performance evaluation is performed .

The remainder of this paper is structured as follows: Section II describes the experiment, Section III outlines the methodology, Section IV presents the results, and Section V summarizes the key findings and future directions.

II. *Experimental Setup and Data Analysis*

The data collection process for this study is described in this section. The tested vehicle was a 2021 Ford Escape Plug-in Hybrid Electric Vehicle (PHEV) from the University of Alberta's fleet which is shown in Figure 1. In this study, 105 tests were conducted, with the vehicle driven along a designated route that is depicted in Figure 1. During each test, an On-Board Diagnostics (OBD-II) device was connected to the vehicle's OBD port to retrieve data from the Electronic Control Unit (ECU), and GPS information.

To address missing data and erroneous data, the raw data was processed using the following steps:

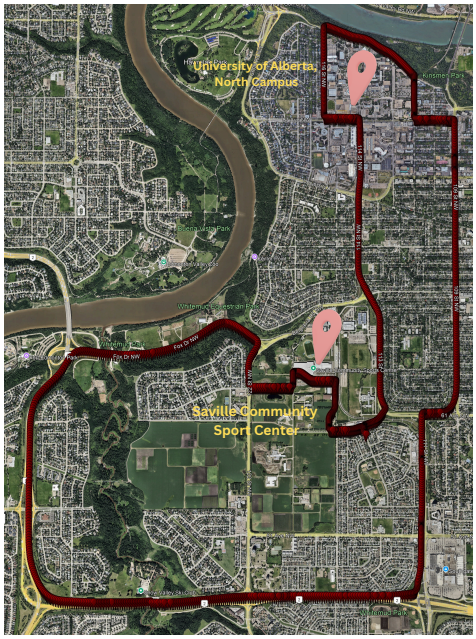

(a) The Test Route

(b) The Test Vehicle

Figure. 1: Overview of the test setup, including the route and the vehicle.

- Missing data points were generated using interpolation methods. Erroneous data points with speed values exceeding the vehicle's physical limits or containing negative values were replaced with realistic estimates. In addition, GPS data points that deviated significantly from the actual route were excluded.
- Acceleration was calculated from the speed data using a central difference, and these values were subsequently incorporated into the dataset.
- The grade profile along the test route was constructed from GPS data (latitude, longitude, and altitude).
- The original data, sampled at 30 Hz, was downsampled to 1 Hz to simplify subsequent processing. This resampling preserves the general characteristics of the data while reducing computational overhead.
- To mitigate noise in the calculated grade (due to inherent GPS inaccuracies), a low pass filter was applied to

smoothen the grade profile.

III. *Markov Chain-based Method*

In this study, a Markov chain-based (MCB) approach to construct a representative driving cycle from experimental data was implemented. In the proposed approach, the vehicle state is defined as a three-dimensional vector

$$s = (v, a, \alpha), \tag{1}$$

where v denotes the vehicle speed, a the acceleration, and α the road grade. The next step in constructing the representative driving cycle using the MCB is the calculation of the state transition matrix which represents the transition between states in the experimental data.

Let the state transition matrix $\mathbf{P} \in \mathbb{R}^{N \times N}$ be defined by

$$P_{ij} = \begin{cases} \frac{n_{ij}}{N_i}, & \text{if } n_{ij} > 0, \\ 0, & \text{otherwise}, \end{cases} \tag{2}$$

where n_{ij} is the number of observed transitions from state s_i to state s_j and

$$N_i = \sum_{j=1}^{N} n_{ij}.$$

Here, the total number of states is given by

$$N = n_v \times n_a \times n_\alpha,$$

with n_v, n_a, and n_α representing the number of bins for speed, acceleration, and road grade, respectively.

Due to the high dimensionality of the state space, most transitions are either very infrequent or unobserved, resulting in a sparse transition matrix. The sparse matrix can be represented as

$$\mathbf{P} = \{(i, j, P_{ij}) \mid P_{ij} = \frac{n_{ij}}{N_i},\ n_{ij} > 0,\ i, j = 1, \ldots, N\}.$$

Alternatively, using the standard basis vectors $\{\mathbf{e}_i\}_{i=1}^{N}$, it can be expressed $\mathbf{P}$ as

$$\mathbf{P} = \sum_{(i,j) \in \mathcal{S}} P_{ij}\, \mathbf{e}_i\, \mathbf{e}_j^{\top}, \tag{3}$$

where $\mathcal{S} = \{(i, j) \mid n_{ij} > 0\}$ denotes the set of index pairs corresponding to the feasible transitions.

This sparse matrix formulation efficiently manages memory usage while capturing the essential transition dynamics of the system.

In the next step, once the transition matrix $\mathbf{P} = [P_{ij}]$ is calculated, the driving cycle is constructed by the Markov chain process. Starting from an initial state s_0, the next state is chosen according to the probability distribution:

$$\Pr(s_{t+1} = s_j \mid s_t = s_i) = P_{ij}. \tag{4}$$

In practice, this selection is implemented using a uniformly distributed random number $u \sim U(0, 1)$ such that

$$s_{t+1} = s_j \quad \text{if} \quad \sum_{k=1}^{j-1} P_{ik} < u \leq \sum_{k=1}^{j} P_{ik}. \tag{5}$$

This iterative process repeats until the constructed driving cycle reaches the desired driving cycle length.

By including the road grade component α in equation (1), the conventional two-dimensional state space is expanded into a three-dimensional space which leads to more realistic and representative driving cycle. Consequently, the transition probability in the context of road grade becomes:

$$\Pr\big((v_{t+1}, a_{t+1}, \alpha_{t+1}) \mid (v_t, a_t, \alpha_t)\big) = P_{ij}, \tag{6}$$

this inclusion of road grade into the state definition and into the state transition matrix ensures the the constructed driving cycle is capturing the road grade dynamics along with dynamics of vehicle speed and acceleration.

By iteratively simulating the Markov chain using (3) to (5), the resulting driving cycle statistically mirrors the dynamic characteristics observed in the real-world experimental data by considering transition probability derived from experimental data in the states in each time step.

The algorithm detailing this simulation process is presented in Algorithm 1, which encapsulates the discretization of the state space, the construction of the sparse transition matrix, and the sequential generation of the driving cycle.

IV. *Results and Discussions*

The results of the MCB methodology for constructing representative driving cycles are presented in two parts. First, the multi-dimensional representative driving cycles, including speed, acceleration, and road grade over time, are detailed in Section IV-A. Second, the impact of road grade on representative driving cycles is analyzed in Section IV-B.

A. Constructed Representative Driving Cycles

Figure 2 shows the constructed representative driving cycle using the iMCB for our collected dataset. The cycle captures key driving dynamics, including variations in speed, acceleration, and road grade, which are critical for accurately simulating vehicle performance. In constructing this cycle, the vehicle speed is discretized into 150 bins, the acceleration into 81 bins, and the road grade into 40 bins, resulting in a detailed representation of the driving behavior. Vehicle speed (in m/s) versus time, with a driving cycle length was set to approximately 2000 seconds, this value was determined based on the average cycle length observed in our experimental data that is shown in Figure 1.

To assess the representativeness of the constructed driving cycle, a set of kinematic fragments from the driving data are computed. These fragments provide quantitative insights into various aspects of driving behavior and are as follows:

- *Average Speed Excluding Idling ($\bar{V}_{EI}$)*: the vehicle speed for data points where the speed exceeds 0.025 m/s, thereby excluding periods of idling.
- *Average Speed ($\bar{V}$)*: The mean speed over the entire dataset, provides a general measure of vehicular motion.
- *Average Positive Acceleration/Negative Acceleration ($\bar{A}_p/\bar{A}_n$)*: is calculated by averaging the acceleration values when they exceed 0.15 m/s^2, or below -0.15 m/s^2.

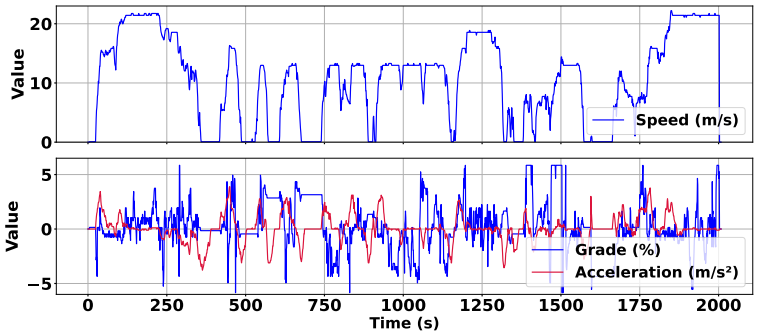

Figure. 2: Constructed driving cycle via MCB method.

Algorithm 1 Driving Cycle Construction using MCB

Input: Driving data D with vehicle speed v_i, acceleration a_i, and road grade α_i, for every i, where $\forall i \in \{1, 2, \ldots, N_c\}$, with N_c as the driving cycle length.
Discretize: Bin v, a, and g into n_v, n_a, and n_α bins.
Define each state as $s = (v, a, \alpha)$, with a total of N states.
Initialize: a sparse transition matrix $\mathbf{P} \in \mathbb{R}^{N \times N}$.
for each observed transition $s_i \to s_j$ in D **do**
  Increment count n_{ij}.
end for
for each state s_i, $i = 1, \ldots, N$ **do**
  Compute $N_i = \sum_{j=1}^{N} n_{ij}$.
  for each state s_j, $j = 1, \ldots, N$ **do**
    if $n_{ij} > 0$ **then**
      Set $P_{ij} \leftarrow \dfrac{n_{ij}}{N_i}$.
    else
      Set $P_{ij} \leftarrow 0$.
    end if
  end for
end for
Initialize driving cycle C with an initial state s_0.
while length$(C) < T$ **do**
  Let the current state be s_i.
  Generate $u \sim U(0, 1)$.
  Select next state s_j satisfying

$$\sum_{k=1}^{j-1} P_{ik} < u \leq \sum_{k=1}^{j} P_{ik}.$$

  Append s_j to C.
end while
return C.
Output: Constructed driving cycle C.

- *Idling Percentage (t_i)*: the vehicle speed is at or below 0.025 m/s as a percentage of total driving cycle time.
- *Cruising Percentage (t_c)*: when the vehicle maintains a steady state, characterized by acceleration values between -0.15 m/s^2 and 0.15 m/s^2 and a speed above 5 m/s as a percentage of total driving cycle time.
- *Positive Acceleration and Negative Acceleration Percentage (t_{ap}, t_{an})*: the total time during which the vehicle is accelerating (acceleration > 0.15 m/s^2) or decelerating (acceleration < -0.15 m/s^2) as a percentage of the total driving cycle time.

The kinematic fragments are used in validating the constructed driving cycle's fidelity to real-world driving behavior. A quantitative comparison between the constructed Representative Driving Cycle (RDC) and the actual driving cycle data is listed in Table I. The MCB constructed cycle exhibits an $\bar{V}_{EI}$ of 10.70 m/s, which has an absolute error of 0.98 m/s. This error is greater than 1 standard deviation (0.50) but within 2 standard deviations. In contrast, the $\bar{V}$ is slightly overestimated at 10.63 m/s compared to the actual 9.82 m/s, resulting in an absolute error of 0.81 m/s, which is greater than 1 standard deviation (0.68) but within 2 standard deviations.

In terms of $\bar{a}_p$ and $\bar{a}_n$, the constructed cycle demonstrates an $\bar{a}_p$ of 1.34 m/s^2 and an $\bar{a}_n$ of -1.32 m/s^2. These values closely match the actual measurements of 1.26 m/s^2 and -1.26 m/s^2, leading to absolute errors of 0.08 and 0.06, respectively. Both errors are within 1 standard deviation ($\sigma_{\bar{a}_p} = 0.101$, $\sigma_{\bar{a}_n} = 0.099$), indicating a high fidelity in capturing acceleration dynamics.

The time metrics further reflect the dynamic driving conditions encountered in the dataset. The percentage of time allocated to acceleration, deceleration, and cruising in the constructed cycle shows absolute errors of 2.57%, 3.11%, and 6.36%, respectively. The error for acceleration percentage (2.57) is slightly above 1 standard deviation (2.07) but within 2 standard deviations. The deceleration percentage error (3.11) is also slightly greater than 1 standard deviation (1.95) but remains within 2 standard deviations. However, the cruising time error (6.36) exceeds 1 standard deviation (3.64), suggesting some deviation in cruise time representation.

On the other hand, the constructed cycle significantly underestimates the idling time, with an absolute error of 10.97%, which is much larger than 2 standard deviations (3.65). This considerable discrepancy in idling may be attributed to the inherent challenges of capturing the stochastic nature of idling events or due to differences in how idling is detected and recorded in the experimental data. Overall, the MCB method demonstrates promising results in replicating key aspects of real-world driving. Certain areas, particularly the idling time,

require further refinement.

Furthermore, the constructed driving cycle exhibits an average computation time of 3.75 hours, which may impede its practical application, particularly in scenarios where rapid analyses of vehicle performance, fuel consumption, and emissions estimation are crucial. Therefore, optimizing the computational efficiency of the MCB approach is an important aspect of future research.

TABLE. I: Comparison of Constructed RDC and Actual Driving Cycle Metrics for Positive Sunny Condition.

Kin. Fragments	Constructed	Actual	Abs. Error	STD
V_{EI} [m/s]	10.7	11.7	0.980	0.500
$\bar{V}$ [m/s]	10.6	9.82	0.810	0.680
$\bar{a}_p$ [m/s^2]	1.34	1.26	0.0800	0.101
$\bar{a}_n$ [m/s^2]	-1.32	-1.26	0.0600	0.0990
t_{ap} [%]	26.8	29.3	2.57	2.07
t_{an} [%]	25.3	28.4	3.11	1.95
t_c [%]	38.9	32.6	6.36	3.64
t_i [%]	4.98	15.9	10.97	3.65

B. Representative Driving Cycle with Road Grade

The impact of road grade incorporation into the representative driving cycle is investigated by comparing the Vehicle Specific Power (VSP) distributions for cycles constructed with and without road grade. The VSP distribution for the cycle constructed without grade consideration, and with road grade is shown in Figure 3. A visual inspection of these figures reveals that the inclusion of road grade not only shifts the overall distribution but also alters its spread, indicating changes in the power demand characteristics of the vehicle.

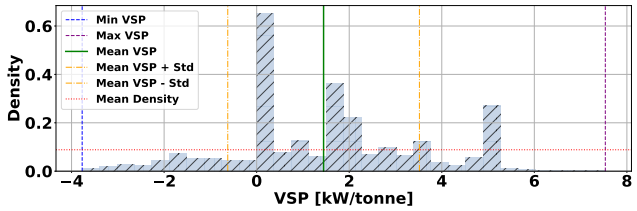

(a)

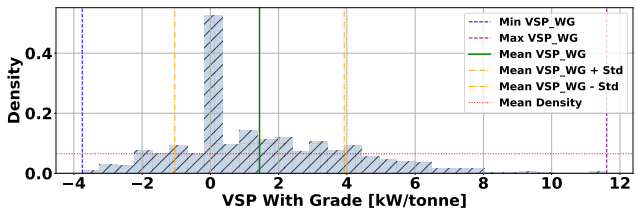

(b)

Figure. 3: The VSP distribution for constructed driving cycles with (a) no grade and (b) grade.

To quantify these differences, Table II presents several statistical measures of the VSP for with and without road grade driving cycles. The results show that the mean VSP changes from 1.45 kW/ton (without grade) to 1.44 kW/ton (with grade), corresponding to an approximate 0.69% decrease. By incorporating road grade, a higher average engine load, likely due to the additional power required to overcome gravitational forces, is obtained. Similarly, the variance in VSP increases from 4.29 to 6.15 (a 43.3% change), indicating a broader distribution in the power demand when road grade is considered. The maximum VSP value increases from 7.53 kW/ton to 11.61 kW/ton (a 54.2% increase), and peak power demands increase when road grade is considered.

In contrast, the minimum VSP values are only marginally affected, shifting from -3.77 kW/ton to -3.75 kW/ton (a 0.53% change), indicating that the lower part of the power distribution is less influenced by road grade. Additionally, the center area density, which represents the most common VSP occurrences, decreases by 22.2% with grade consideration, while the center area VSP value itself remains unchanged at 1.44 kW/ton.

TABLE. II: Updated Statistics on the VSP with and without Road Grade Consideration for the Large Dataset. Units are in kW/ton.

Metric	Without Grade	With Grade	Δ (%)
Mean (VSP)	1.45	1.44	-0.690
Variance (σ_{VSP})	4.29	6.15	43.3
Min (VSP_{Min})	-3.77	-3.75	0.530
Max (VSP_{Max})	7.53	11.6	54.2
Center Area [Density]	0.0900	0.0700	-22.2
Center Area [VSP]	1.44	1.44	0.000

The significant changes in the mean, variance, and maximum VSP, when road grade is incorporated, highlight the additional power requirements imposed by road slopes. Moreover, the altered distribution, evidenced by the decrease in center area density and the unchanged center area VSP, underscores the need to consider road grade effects in order to achieve a more realistic representation of vehicle performance, which is critical for accurate analyses of fuel consumption and emissions in real driving cycles.

V. Conclusions

A representative driving cycle construction method integrating vehicle speed, acceleration, and road grade from real-world data is presented. This method employs a sparse transition matrix that enables the large state space consideration. This expanded state space allows the method to include road grade transitions in the experimental data in the process of driving cycle construction, resulting in a more representative driving cycle.

Our findings confirm that a driving cycle that incorporates vehicle speed, acceleration, and road grade provides an improved basis for performance evaluation, fuel consumption estimation, and emission analysis, as the results show that by incorporating road grade, the mean Vehicle Specific Power (VSP) changes by 0.69% (from 1.45 to 1.44 kW/tonne), while its variance increases by 43.3% (from 4.29 to 6.15).

Although the current implementation of the iMCB approach requires an average runtime of 3.75 hours, a challenge

for rapid analyses, this study lays a robust foundation for future algorithmic optimizations. Therefore, future research will focus on further enhancing computational efficiency and extending the framework to include additional variables such as weather conditions and cold climate effects. These advancements are essential for developing next-generation, eco-friendly transportation systems and achieving more accurate vehicle simulations.

ACKNOWLEDGEMENTS

We gratefully acknowledge the support of Energy Management and Sustainable Operations (EMSO) of the University of Alberta and Environment and Climate Change Canada, under the Climate Action and Awareness Fund, for supporting this work.

REFERENCES

[1] Tofigh, M., Kharazmi, A., Smith, D. J., Koch, C. R., and Shahbakhti, M., "Temporal dilated convolution and nonlinear autoregressive network for predicting solid oxide fuel cell performance," *Engineering Applications of Artificial Intelligence*, vol. 136, 2024, 108994.

[2] United Nations, "Causes and effects of climate change," 2024. [Online]. Available: https://www.un.org/en/climatechange/science/causes-effects-climate-change. [Accessed: December 19, 2024].

[3] European Commission, Joint Research Centre (JRC), "Edgar - emissions database for global atmospheric research, report 2024," 2024. [Online]. Available: https://edgar.jrc.ec.europa.eu/report_2024. [Accessed: December 19, 2024].

[4] Environment and Climate Change Canada, "Greenhouse gas emissions: Sources and sinks in Canada - executive summary," 2024. [Online]. Available: https://www.canada.ca/en/environment-climate-change/services/climate-change/greenhouse-gas-emissions/sources-sinks-executive-summary-2024.html. [Accessed: December 19, 2024].

[5] U.S. Environmental Protection Agency, "Regulations for onroad vehicles and engines," 2024. [Online]. Available: https://www.epa.gov/regulations-emissions-vehicles-and-engines/regulations-onroad-vehicles-and-engines. [Accessed: December 19, 2024].

[6] Government of Canada, "Regulations respecting reduction in the release of greenhouse gases and air pollutants from vehicles and engines," 2024. [Online]. Available: https://pollution-waste.canada.ca/environmental-protection-registry/regulations/view?Id=119. [Accessed: December 19, 2024].

[7] Tofigh, M., Fakouri Hasanabadi, M., Smith, D., Kharazmi, A., Hanifi, A. R., Koch, C. R., and Shahbakhti, M., "Control-Oriented Modeling of a Solid Oxide Fuel Cell Affected by Redox Cycling Using a Novel Deep Learning Approach," *Journal of Dynamic Systems, Measurement, and Control*, vol. 147:2, 2025, 021006.

[8] C. Pan, Y. Tao, L. Wang, H. Li, and J. Yang, "Fuzzy energy management strategy for electric vehicle combining driving cycle construction and air-conditioning load identification," *Advances in Mechanical Engineering*, vol. 13, 2021, Art. no. 1687814021994381.

[9] O. A. Huzayyin, H. Salem, and M. A. Hassan, "A representative urban driving cycle for passenger vehicles to estimate fuel consumption and emission rates under real-world driving conditions," *Urban Climate*, vol. 36, 2021, Art. no. 100810.

[10] G. Fontaras, N.-G. Zacharof, and B. Ciuffo, "Fuel consumption and CO2 emissions from passenger cars in Europe—Laboratory versus real-world emissions," *Progress in Energy and Combustion Science*, vol. 60, 2017, pp. 97–131.

[11] A. Alam and M. Hatzopoulou, "Modeling transit bus emissions using MOVES: Comparison of default distributions and embedded drive cycles with local data," *Journal of Transportation Engineering, Part A: Systems*, vol. 143, 2017, Art. no. 04017049.

[12] S. H. Kamble, T. V. Mathew, and G. K. Sharma, "Development of real-world driving cycle: Case study of Pune, India," *Transportation Research Part D: Transport and Environment*, vol. 14, 2009, pp. 132–140.

[13] L. F. Quirama, M. Giraldo, J. I. Huertas, and M. Jaller, "Driving cycles that reproduce driving patterns, energy consumptions and tailpipe emissions," *Transportation Research Part D: Transport and Environment*, vol. 82, 2020, Art. no. 102294.

[14] M. Giraldo, L. F. Quirama, J. I. Huertas, and J. E. Tibaquirá, "The effect of driving cycle duration on its representativeness," *World Electric Vehicle Journal*, vol. 12, 2021, p. 212.

[15] D. Förster, R. B. Inderka, and F. Gauterin, "Data-driven identification of characteristic real-driving cycles based on k-means clustering and mixed-integer optimization," *IEEE Transactions on Vehicular Technology*, vol. 69, 2019, pp. 2398–2410.

[16] Q. Wang, H. Huo, K. He, Z. Yao, and Q. Zhang, "Characterization of vehicle driving patterns and development of driving cycles in Chinese cities," *Transportation Research Part D: Transport and Environment*, vol. 13, 2008, pp. 289–297.

[17] P. Lipar, I. Strnad, M. Česnik, and T. Maher, "Development of urban driving cycle with GPS data post-processing," *Promet- Traffic&Transportation*, vol. 28, 2016, pp. 353–364.

[18] M. Zhang, S. Shi, W. Cheng, Y. Shen, and W. Cao, "Using the AMCE algorithm to high-efficiently develop vehicle driving cycles with road grade," *IEEE Access*, vol. 7, 2019, pp. 160449–160458.

[19] Y. Cui, H. Xu, F. Zou, Z. Chen, and K. Gong, "Optimization-based method to develop representative driving cycle for real-world fuel consumption estimation," *Energy*, vol. 235, 2021, Art. no. 121434.

[20] P. Nyberg, E. Frisk, and L. Nielsen, "Generation of equivalent driving cycles using Markov chains and mean tractive force components," *IFAC Proceedings Volumes*, vol. 47, 2014, pp. 8787–8792.

[21] B. Škugor and J. Deur, "Delivery vehicle fleet data collection, analysis and naturalistic driving cycles synthesis," *International Journal of Innovation and Sustainable Development*, vol. 10, 2016, pp. 19–39.

[22] X. Jia, H. Wang, L. Xu, Q. Wang, H. Li, Z. Hu, J. Li, and M. Ouyang, "Constructing representative driving cycle for heavy-duty vehicle based on Markov chain method considering road slope," *Energy and AI*, vol. 6, 2021, Art. no. 100115.

[23] X. Zeng and J. Wang, "A parallel hybrid electric vehicle energy management strategy using stochastic model predictive control with road grade preview," *IEEE Transactions on Control Systems Technology*, vol. 23, 2015, pp. 2416–2423.

[24] S. Lopp, E. Wood, and A. Duran, "Evaluating the impact of road grade on simulated commercial vehicle fuel economy using real-world drive cycles," Technical Report, *SAE Technical Paper*, 2015.